04,14

Impact damage of cement rock subjected to short-time uniaxial compressing

© A.G. Kadomtsev, I.P. Shcherbakov, A.E. Chmel¶

Ioffe Institute,
St. Petersburg, Russia

¶ E-mail: chmel@mail.ioffe.ru

Received January 23, 2025
Revised February 10, 2025
Accepted February 12, 2025

An application of high hydrostatic pressure is the effective procedure decreasing porosity and conditioning the mechanical properties cement rock (CR). In the present paper, the effect of the uniaxial compression of the aging-treated CR on its impact-strength in the direction orthogonal to the applied pressure was investigated. The test geometry falls in line with the distribution of outer forces in built structures, where a constant vertical load is combined with the horizontal dynamic action of forces of various origine. The localized damage development in laboratory samples was controlled by the acoustic emission method, which is sensitive to the CR structure destruction at the micromechanical level. It was revealed that a cycle of static loading modifies the character of the energy yield resulted from the localized impact produced in a loaded and off-loaded sample in dependence of the applied vertical pressure.

Keywords: axial pressure, repeated load, acoustic emission.

DOI: 10.61011/PSS.2025.02.60676.17-25

1. Introduction

Porosity is one of the most important properties of cement rock (CR). Hydrostatic pressure applied at the hardening stage exerts an effective impact on porosity in order to improve mechanical properties of CR [1]. At the same time, during operation of structures, CR might be exposed to man-made (explosions, mining) and natural (volcanic activity, earthquakes) shock waves [2] and to periodic loads [3] (tides, hurricanes). Compressive pressures of finished porous product may potentially modify its strength properties to a certain extent [4]. This study determined the influence of uniaxial compression of laboratory CR samples on an impact oriented orthogonally to compression, which is an underinvestigated field.

Local point impact fracture pattern was evaluated by the acoustic emission (AE) method that is used to determine the microcrack formation/accumulation energy yield in static and dynamic (in particular impact) loading [5–8]. The experiments simulated two types of situations: impact damage of a surface directly on a compressed sample and on a sample after static load removal. Loading geometry was chosen in accordance with the mechanical force distribution in building structures, whose lower members were compressed vertically and side surfaces were under dynamic loading.

2. Samples and equipment

Naturally hardened M400 CR samples, $10 \times 10 \times 40$ mm, were placed under the GE-TPO10 bench-type hydraulic press for compression along the largest dimension of the plate (Figure 1). A pendulum

Figure 1. General view of a system for AE generation with impact damage of an uniaxially compressed CR sample.

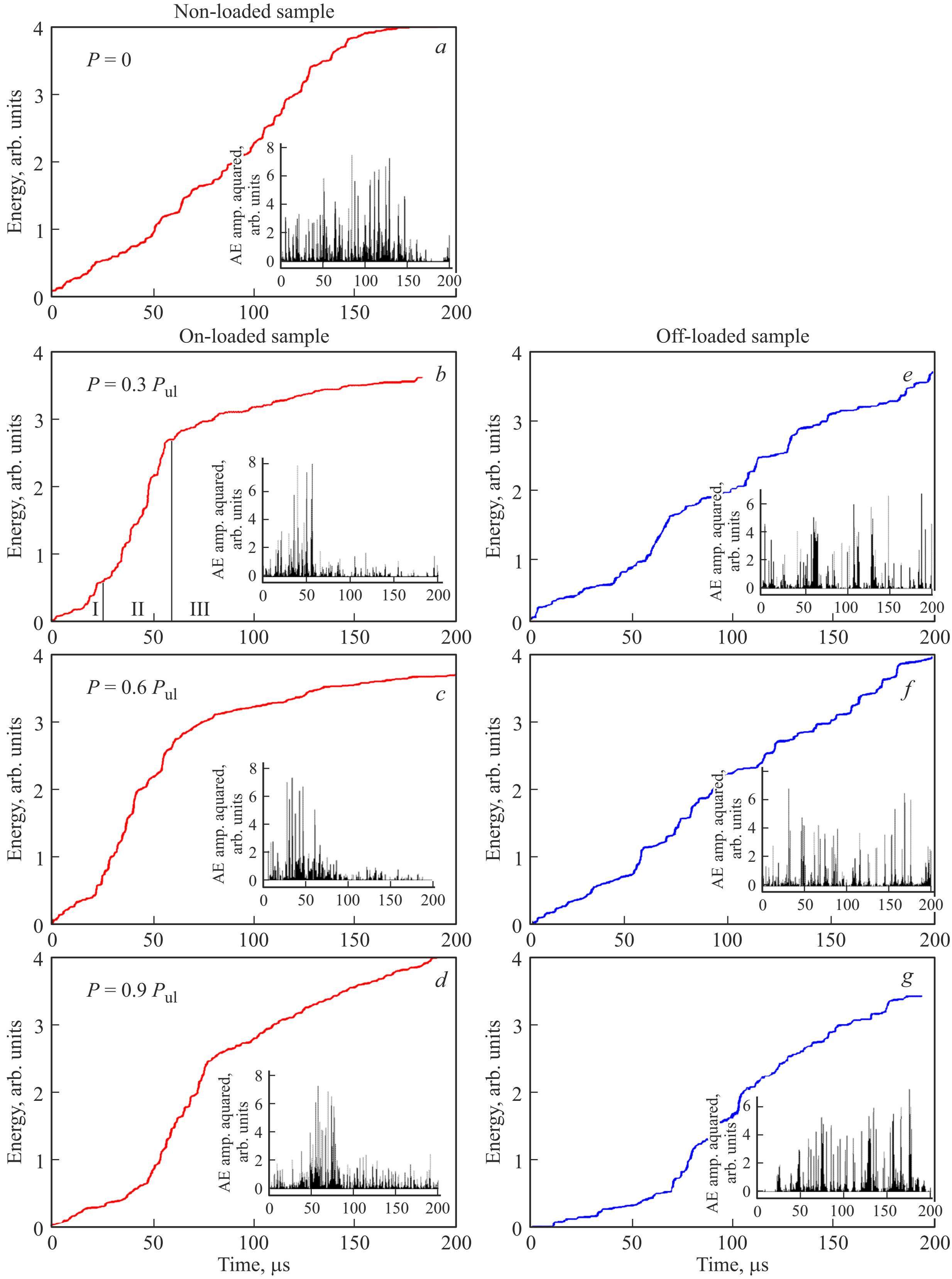

Figure 2. AE activity and microcrack formation energy yield kinetics in M400 CR during point impact damage of uniaxially compressed samples. Explanations of alphabetical symbols in the text.

machine with sharp die was used to make a 0.1 J impact on the sample orthogonally to the axial static load to generate local damage of a $\sim 1\,\mathrm{mm}^2$ surface.

Nominal strength of the M400 concrete is about 40 MPa, but may be much higher than this value in laboratory conditions [1]. Therefore, ultimate (threshold) compression load without impact load P_{ul} was preliminary measured for particular samples. Current impact load P was measured step-by-step from 0 to $P = 0.3P_{\mathrm{ul}}$; $0.6P_{\mathrm{ul}}$; $P = 0.9P_{\mathrm{ul}}$. In each compression cycle, the sample was exposed to an axial load lower than 3 min. PZT ceramic piezoelectric transducer installed on a side surface of the sample recorded time scans within 400−600 kHz of AE induced by microcracking in the CR material [9]. AE generation was recorded during 2 ms with time resolution of 40 ns.

3. Results and discussion

Insets in Figure 2 show scans of AE signals induced by the test machine impact on samples before compression loading (Figure 2, *a*), in axial compression pressure P (Figure 2, *b*−*d*) and off-loaded samples (again $P = 0$) (Figure 2, *e*−*g*). The insets show that the active AE generation period decreases drastically when the compression load is applied (Figure 2, *b*−*d*), which may be due to the decrease in CR porosity. In [1], it was shown that the M400 concrete porosity decreased approximately by half when pressure 60 MPa was applied; porosity variation in higher compression was insignificant. After removal of the axial load, scan time is approximately restored (Figure 2, *e*−*g*).

Acoustic pulse energy E is proportional to the squared amplitude A: $E \propto A^2$. Energies of successive impact-induced pulses were summed. Energy yield curve profiles plotted during test machine impact on the surface at pressure on the sample $P = 0$; $0.3P_{\mathrm{ul}}$; $0.6P_{\mathrm{ul}}$; and $0.9P_{\mathrm{ul}}$ vary successively as the static pressure increases. With zero load, time dependence of total AE energy accumulation is almost linear, but when axial compression is applied, the dependence transforms into a complex curve that includes three elements shown in Figure 2, *b*: initial segment with a gentle slope (zone I); segment with increased crack accumulation rate (zone II); and finish segment with decaying emission (zone III).

Accumulation of impact-induced microcracks is determined by the distribution of a limited number of initial structural defects in CR that reduce material strength. Their fracture is followed by low-energy AE pulse release — the accumulation curve has a gently sloping segment (I). The initial segment is most pronounced at the maximum load $P = 0.9P_{\mathrm{ul}}$ (Figure 2, *d*), because the „reservoir“ of relatively weak spots expands on the approach to threshold fracture. As the „weak spots“ deplete, fracture of the main CR structure starts, with release of high-energy pulses — a short CR burst occurs by increasing the accumulation curve slope (II). At the last load stage (III), the curve slope decreases again with shock wave relaxation.

After removal of static load, the same samples were exposed to impact. Emphasis is made on a longer AE scan time than that for compressed sample impact (Figure 2, *e*−*g*). This detail indicates a relaxation of sample material structures exposed to static loading cycle.

The total AE pulse energy accumulation curves from off-loaded samples exposed to $P = 0.3P_{\mathrm{ul}}$ and $P = 0.6P_{\mathrm{ul}}$ showed only considerable decrease in curve slope compared with the curve of a sample not exposed to compression (Figure 2, *a*); slope reduction indicates some material hardening due to the disappearance of a part of „weak spots“. However, when the maximum test machine pressure $P = 0.9P_{\mathrm{ul}}$ is applied, the off-loaded sample energy release curve appeared to be close to that for static load test samples. This indicates that residual mechanical damage of CR structure occurs at the last (critical) compression cycle.

4. Conclusion

The acoustic emission (AE) method showed that the applied static axial load considerably alters the impact fracture pattern of M400 CR by displaying three different energy release modes. Sample unloading after compression by 0.3 and 0.6 from the global fracture threshold mainly follows the AE pulse time pattern at $P = 0$, but with a lower energy yield, which indicates a particular degree of material hardening. After the cycle of compression by 0.9 from the fracture threshold, irreversible changes were detected in the material structure.

Conflict of interest

The authors declare that they have no conflict of interest.

References

[1] V.I. Betekhtin, A.N. Bakhtibayev, A.G. Kadomtsev, D.A. Imanbekov. Tsement i ego primenenie *5–6*, 16 (1991). (in Russian).

[2] J. Pachman, D.J. Chapman, M. Foglar, M. Künzel, W.G. Proud. Int. J. Impact Eng. **183**, 104787 (2024). https://doi.org/10.1016/j.ijimpeng.2023.104787

[3] J.H. Kurz, F. Finck, C.U. Grosse, H.W. Reinhardt. Struct. Health Monit. **5**, 69 (2006). https://doi.org/10.1177/1475921706057983

[4] C. Lian, Y. Zhuge, S. Beecham. Constr. Build. Mater. **25**, *11*, 4294 (2011). https://doi.org/10.1016/j.conbuildmat.2011.05.005

[5] E. Verstrynge, G. Lacidogna, F. Accornero, A. Tomor. Constr. Build. Mater. **268**, 121089 (2021). https://doi.org/10.1016/j.conbuildmat.2020.121089

[6] V.N. Saveliev, Kh.F. Makhmudov. ZhTF **90**, *1*, 143 (2020). (in Russian). https://doi.org/10.21883/JTF.2020.01.48676.74-19 [V.N. Savel'ev, Kh.F. Makhmudov. Tech. Phys. **65**, *1*, 133 (2020)]

[7] V.P. Surzhikov, N.N. Khorsov. Tech. Phys. **60**, *1*, 148 (2015).

[8] F. Sagasta, M.E. Zitto, R. Piotrkowski, A. Benavent-Climent, E. Suarez, A. Gallego. MSSP **102**, 262 (2018). https://doi.org/10.1016/j.ymssp.2017.09.022

[9] S.G. Nikolsky. Inzhenerno-stroitelny zhurnal **2**, 39 (2008). (in Russian).

Translated by E.Ilinskaya